Visible – light driven systems: effect of the parameters affecting hydrogen production through photoreforming of organics in presence of Cu_2O/TiO_2 nanocomposite photocatalyst

M. Muscetta [(1),*], L. Clarizia [(1),*], M. Race[(2)], R. Andreozzi[(1)], R. Marotta[(1)], I. Di Somma[(3)]

[(1)] Dipartimento di Ingegneria Chimica, dei Materiali e della Produzione Industriale, Scuola Politecnica e delle Scienze di Base, Università di Napoli Federico II, Italia.

[(2)] Dipartimento di Ingegneria Civile e Meccanica, Università degli Studi di Cassino e del Lazio Meridionale, Italia.

[(3)] Istituto di Scienze e Tecnologie per l'Energia e la Mobilità Sostenibili (CNR), Napoli, Italia.

**Corresponding authors: marica.muscetta@unina.it (M. Muscetta);*

laura.clarizia2@unina.it (L. Clarizia).

Keywords: green hydrogen, photoreforming, ball milling, cuprous oxide, solar photocatalysis

Abstract

Several studies have shown that combining TiO_2 and Cu_2O enhances the photocatalytic activity of the material by generating a heterojunction capable of extending the light absorption in the visible and reducing the electron-hole recombination rate. Ball milling has been chosen as an alternative methodology for photocatalyst preparation, among the several techniques documented in the literature review. The results of a previously reported investigation enabled the identification of the most effective photocatalyst that can be prepared for hydrogen generation by combining Cu_2O and TiO_2 (i.e., 1%wt Cu_2O in TiO_2 photocatalyst prepared by ball-milling method at 200 rpm and 1 min milling time). To optimize photocatalytic hydrogen generation in the presence of the greatest photocatalyst, the effects of (i) sacrificial species and their concentration, (ii) temperature, and (iii) pH of the system are taken into account, resulting in a light-to-chemical energy efficiency of 8% under the best-tested conditions. Last but not least, the possibility of using the present photocatalytic system under direct solar light irradiation is evaluated: the results indicate that nearly 60% of the hydrogen production recorded under sunlight can be attributed to the visible component of the solar spectrum, while the remaining 40% can be attributed to the UV component.

Preprints (www.preprints.org) | NOT PEER-REVIEWED | Posted: 27 January 2023 doi:10.20944/preprints202301.0499.v1

Introduction

Due to global environmental difficulties and the depletion of fossil resources, sustainable energy generation is one of the most important tasks of this century [1]. Hydrogen is a viable alternative energy carrier because of its stability, abundance on Earth's surface, and lack of greenhouse gas emissions [2–7]. Due to its renewability, the use of solar energy to make hydrogen is an appropriate technique for meeting the energy demand [4,8–13]. Photoreforming of organics in the aqueous phase [14–16] is an emerging technique able to combine wastewater treatment and energy production. The creation of visible–light active and stable photocatalytic/photoelectrocatalytic materials is now the greatest obstacle for many researchers, despite a large number of photocatalysts suggested for hydrogen production [17–19]. Among the techniques to improve the photocatalytic activity of the photocatalysts, many researchers have proposed the combination of semiconductors, such as TiO_2, with other materials capable of extending the visible light absorption to the visible range [20–23]. The heterojunction formation by combining TiO_2 and Cu_2O is a viable route to improve solar light utilization [24–27]. Among the different techniques reported in literature findings to prepare Cu_2O/TiO_2 composite material, a simple and industrially practicable ball milling procedure to dryness was selected as an alternate strategy for preparing photocatalysts in our recent study [28]. The results of the previous study allowed the selection of the best photocatalyst for hydrogen generation prepared by mixing Cu_2O and TiO_2 (i.e., 1%wt. Cu_2O in TiO_2 photocatalyst material prepared through ball milling method at a rotation rate of 200 rpm and milling time of 1 min). To optimize the photocatalytic hydrogen production in presence of the best-performing photocatalyst, the effect of the following variables on the hydrogen production is herein investigated:

- Concentration of the sacrificial species;
- Type of sacrificial species used;
- Temperature and pH of the system;
- Photoefficiency under direct sunlight irradiation.

The quantum yield and the light-to-chemical energy are estimated under the optimal conditions seen based on the data.

Preprints (www.preprints.org) | NOT PEER-REVIEWED | Posted: 27 January 2023 doi:10.20944/preprints202301.0499.v1

Material and methods

1.1. Preparation of the photocatalyst

The synthesis of the photocatalyst is performed by following the procedure reported by Muscetta et al. [28], in which the catalyst is completely characterized. A fixed amount of TiO_2 (1500 mg) is mixed in the agate milling tank (PM100, RETSCH), with agate balls and a fixed amount of Cu_2O (150 mg), fixing the rotation rate to 200 rpm and the milling time to 1 minute. In the following sections, the photocatalytic material used will be named (1%wt) Cu_2O/TiO_2.

1.2. Photocatalytic tests and analytical determination

All the materials used in the present investigation are reported in the Supplementary materials. Photocatalytic tests are performed as in [28] (see Figure 1 (A,B) for the schematic illustration of the experimental setup). The Supplemental materials also include a full explanation of the reactor. A UV cutoff solution ($NaNO_2$ 0.5 M) is pumped through the quartz sleeve to allow the investigation of the photocatalytic activity under visible light conditions (λ>400 nm), as reported by others [29]. To perform a typical experimental run, 210 mg of Cu_2O-TiO_2catalyst are suspended in a doubly distilled aqueous solution (V=0.3 L), at fixed pH and concentration of the sacrificial species (0 ÷ 2.5 M). A N_2 stream is bubbled into the solution starting 40 minutes before inserting the photocatalyst to prevent the interaction between dissolved oxygen and copper species or photogenerated electrons. The effect of the temperature was assessed by increasing the temperature of the system up to 80°C (at this temperature a condenser was located on the reactor to prevent the evaporation of the organic species). To test the effect of pH, in some runs the solution pH is corrected to selected values by adding a diluted solution of KOH or $HClO_4$.

The suspension, containing a fixed concentration of the sacrificial agent (2.5 M) and a fixed amount of the photocatalytic material (700 ppm), was exposed to solar radiation (See the Figure 1 (B) for the schematic illustration of the experimental set – up) to evaluate the photoefficiency of the system under solar light irradiation in selected runs. These runs were carried out in early September 2021 in Naples (40° 50’ 0” N, 14° 15’ 0” E), between the hours 11.00 and 13.00 under clear sky conditions. To evaluate the separate contribution of the UV and visible radiation ranges in hydrogen production, some photocatalytic runs are carried out by employing a cut-off filter to eliminate radiations with wavelengths less than 400 nm.

Preprints (www.preprints.org) | NOT PEER-REVIEWED | Posted: 27 January 2023 doi:10.20944/preprints202301.0499.v1

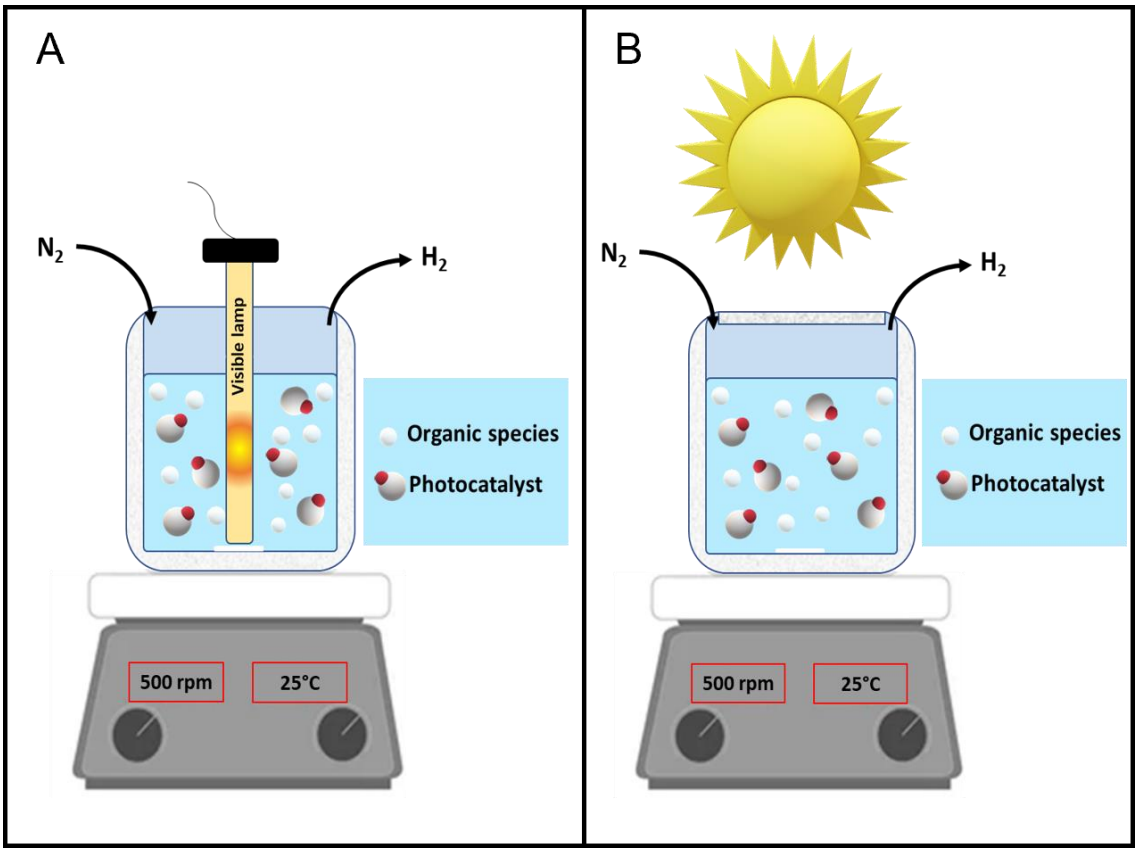

Figure 1. Schematic illustration of the annular batch reactor experimental set-up for the experiments conducted (A) under artificial UV and/or Visible light source and (B) under solar irradiation.

Hydrogen estimation is carried out as reported elsewhere [28,30] The pH of the solution is measured using an Orion 420 p pH–meter (Thermo).

Preprints (www.preprints.org) | NOT PEER-REVIEWED | Posted: 27 January 2023 doi:10.20944/preprints202301.0499.v1

Results and discussions

Effect of organic concentration

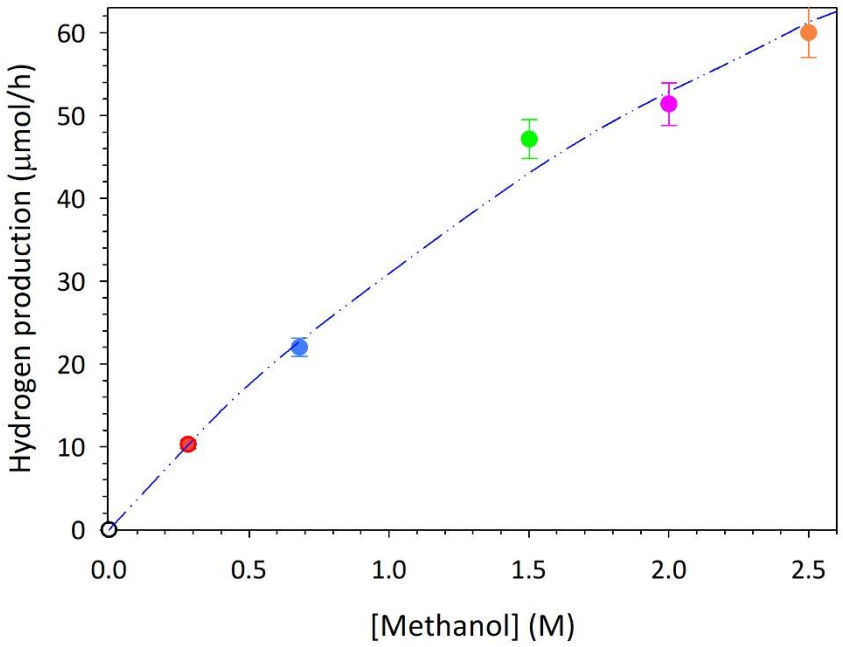

Figure 2. Hydrogen evolution rate at different organic concentrations (methanol). Experimental conditions: V=0.30 L; T=35 °C; P=1atm; pH≈8.5; $C_{(1\%wt.)Cu2O/TiO2}$ = 700 ppm.

The effect of the different parameters affecting the preparation stage of the photocatalyst in the presence of methanol was previously discussed [28]. The influence of methanol concentration on the photocatalytic generation of hydrogen is herein explored. The main results are reported in Figure 2. The reaction rate observed during the photocatalytic runs at varying organic concentrations is properly described by a Langmuir–Hinshelwood model. The adsorbed species concentration may be thus calculated through the equilibrium reaction r.1 and the equation eq.1, in which K_{ads} (M^{-1}) is the adsorption equilibrium constant and θ_{free} is the concentration of free active sites on the catalyst surface:

$$CH_3OH + \theta_{free} \overset{K_{ads}}{\longleftrightarrow} CH_3OH_{ads} \qquad \text{r. 1}$$

$$K_{ads} = \frac{[CH_3OH_{ads}]}{\theta_{free}[CH_3OH]} \qquad \text{eq. 1}$$

Preprints (www.preprints.org) | NOT PEER-REVIEWED | Posted: 27 January 2023 doi:10.20944/preprints202301.0499.v1

To obtain a value of the adsorption constant (K_{ads}) for methanol over the Cu_2O/TiO_2 composite photocatalyst, the following Langmuir–Hinshelwood–type model describing hydrogen generation rate is adopted (eq.2):

$$r_{H_2} = k'' \frac{K_{ads}[CH_3OH]}{1+K_{ads}[CH_3OH]} \qquad \text{eq.2}$$

Where $k''=k' \cdot \theta_t$ (k' being the kinetic constant) and K_{ads} are the apparent kinetic constant of substrate oxidation and the organic adsorption constant, respectively. θ_t (M) is the concentration of total active site on the catalyst surface for a fixed catalyst load q(g/L). The term θ_t is calculated through the following equation (eq. 3):

$$\theta_t = N \cdot q \qquad \text{eq.3}$$

where N is the total moles of active sites per unit mass of catalyst (mol/g).

Starting from eq.3 and plotting the reciprocal of the hydrogen reaction rate versus the reciprocal of the organic concentration (Figure 3), a linear trend is observed, from which it was possible to obtain a suitable value for K_{ads}. By following the optimization procedure reported elsewhere [30], a value of 0.22 M^{-1} is obtained in presence of the best photocatalyst tested when methanol is used as a scavenger. This value resulted in accordance with those reported in literature for similar systems in presence of the same organic compound [31].

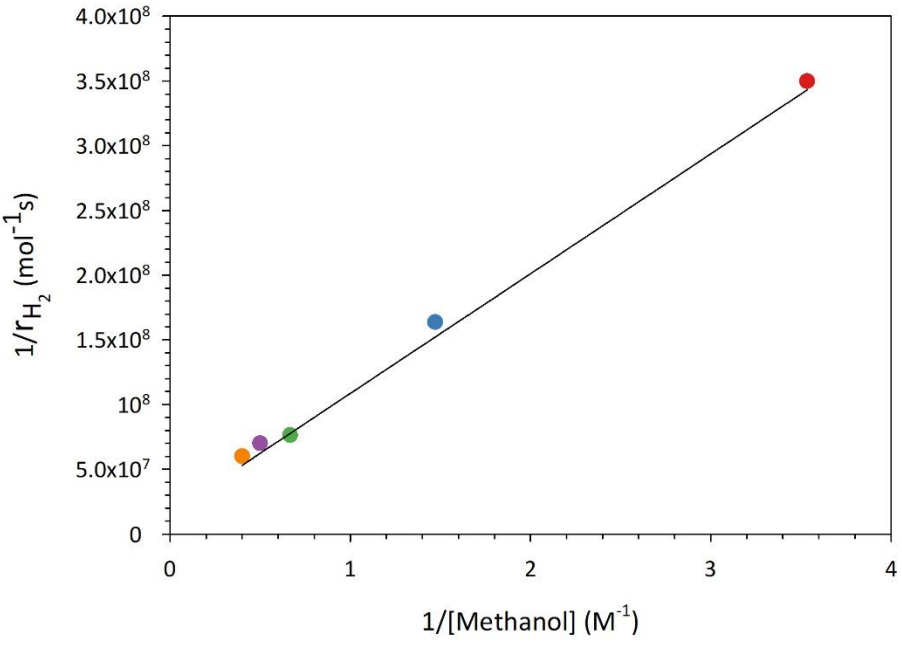

Preprints (www.preprints.org) | NOT PEER-REVIEWED | Posted: 27 January 2023 doi:10.20944/preprints202301.0499.v1

Figure 3. Reciprocal of the hydrogen production vs the inversus of the organic concentration. Experimental conditions: V=0.30 L; T=35 °C; P=1atm; pH≈8.5; $C_{(1\%wt.)Cu2O/TiO2}$ = 700 ppm.

Effect of pH

Some authors have reported a considerable effect of the suspension pH on the photocatalytic hydrogen generation for different photocatalytic materials and scavengers [27,30,32,33]. To evaluate the effect of this variable on the photoactivity, several runs are carried out at varying the solution pH. Figure 4 reports the mean hydrogen production rate collected at different pH values. A higher reactivity may be recognized under alkaline conditions, whereas negligible activity is recorded at acidic conditions (data not shown). Despite the great number of studies in the literature survey focusing on the effect of pH, only few authors have attempted to explain the correlation between solution pH and photocatalytic activity [30,34–36]. The surface properties of the photocatalyst, its stability in the aqueous solution, the shift of the band gap, and the molecular properties of the sacrificial agent should be considered to understand the phenomenon.

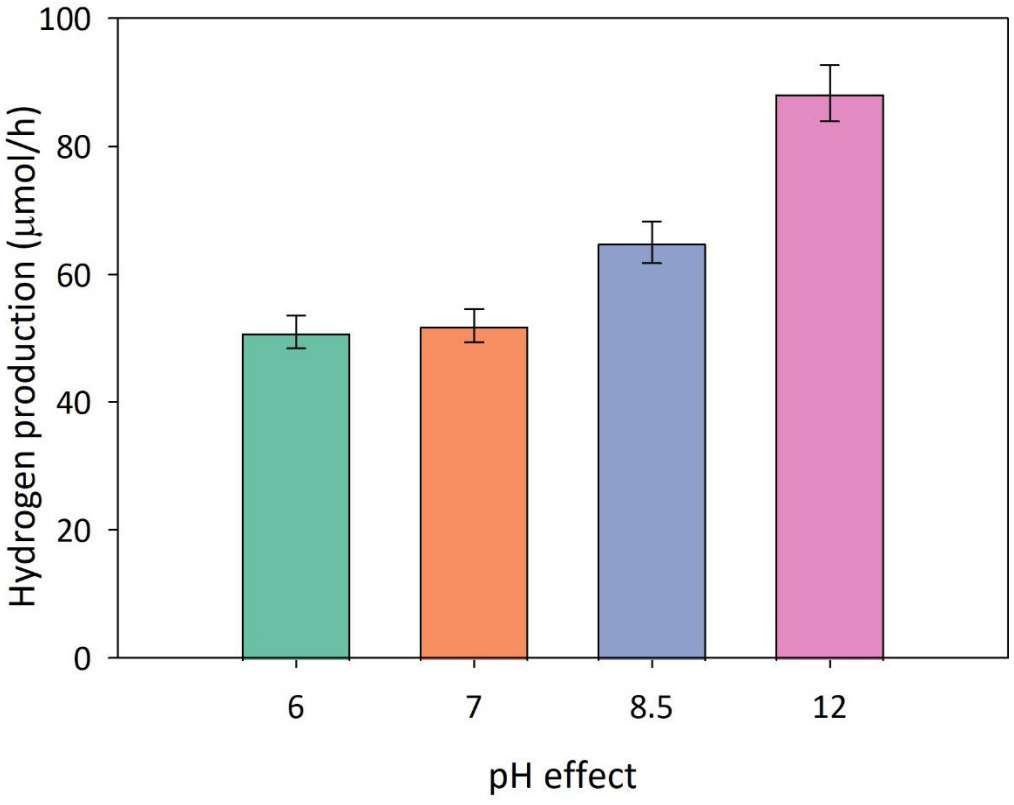

Preprints (www.preprints.org) | NOT PEER-REVIEWED | Posted: 27 January 2023 doi:10.20944/preprints202301.0499.v1

Figure 4. Hydrogen evolution rate at varying the pH of the suspension. Experimental conditions: V=0.30 L; P=1 atm; T=35°C; [Methanol] = 2.5 M; $C_{(1\%wt.)Cu2O/TiO2}$ = 700 ppm; visible range.

The following remarks should be considered to underpin the present photocatalytic outcomes:

(i) The stability of the copper species on the surface of TiO_2 particles is affected by the pH. In particular, lower stability is recorded by several authors under acidic conditions [34,37,38].

(ii) About Methanol (i.e., the sacrificial agent), has a pK_a value of 15.0 [39]. Thus, methanol is present in non-dissociated form for all the pH values tested (See the Figure 5).

(iii) The pH_{zpc} of TiO_2 is about 6.25 [40], Thus, a high concentration of negative charges is recorded on the catalyst surface under alkaline conditions (See the Figure 5) able to promote the interaction between substrate and catalyst surface.

(iv) Negative charges on the catalyst surface (under alkaline conditions) reduce particle agglomeration [41].

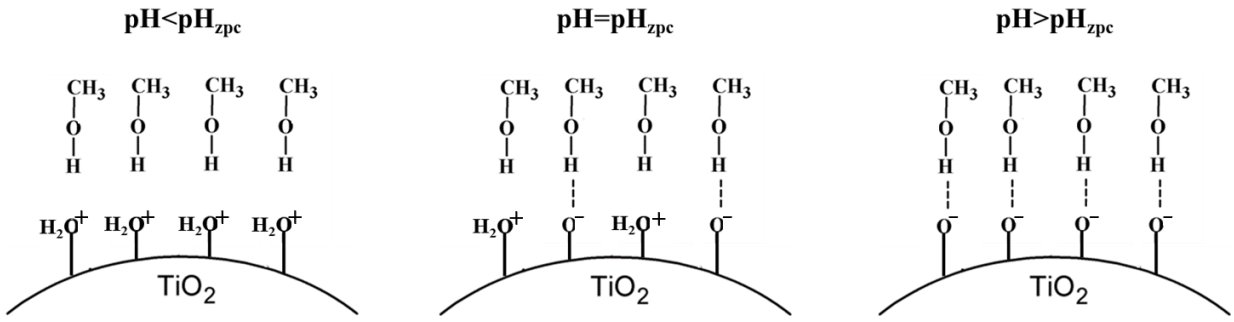

Figure 5. Schematic illustration of adsorption conditions of methanol on the photocatalytic Titania surface at different pH values.

Based on the above considerations, the greater photocatalytic activity in alkaline conditions may be attributed to (i) the presence of stable copper species involved in visible light-induced hydrogen generation and (ii) the more efficient adsorption of the organic compounds.

Preprints (www.preprints.org) | NOT PEER-REVIEWED | Posted: 27 January 2023 doi:10.20944/preprints202301.0499.v1

Effect of temperature

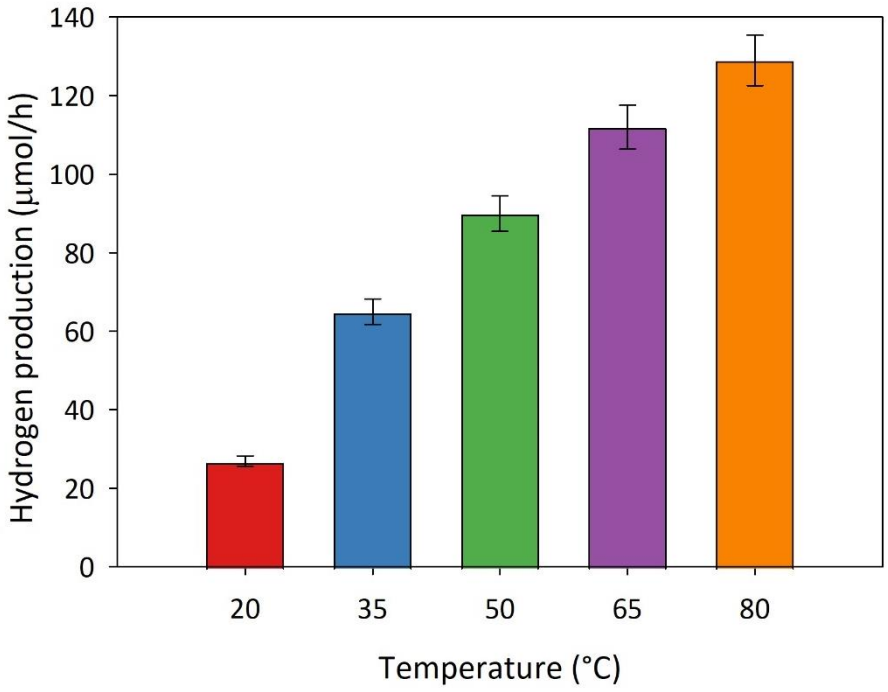

Figure 6. Hydrogen evolution rate at varying the temperature of the system. Experimental conditions: V=0.30 L; P=1 atm; pH≈8.5; [Methanol] = 2.5 M; $C_{(1\%wt.)Cu2O/TiO2}$ = 700 ppm; visible range.

Photocatalytic processes are generally reported to be poorly influenced by the temperature, as the electron-hole generation mainly depends on the radiation intensity [42]. However, the temperature may improve the activity of the system, being able to (*i*) increase the reaction rate of the hydrogen generation and *(ii)* improve the product desorption from the catalyst[43]. Thus, temperature helps hydrogen generation reaction compete more effectively with charge carries recombination, as reported by different authors [44–46]. For this reason, some experimental runs are performed varying the temperature of the suspension between 20°C and 80°C, in presence of methanol as a scavenger. The main results are reported in Figure 6. As clearly sown by the diagram, when the temperature increases from 20°C to 80°C, the hydrogen production rate achieves a value about 4.5 times higher than that obtained at the lowest temperature, thus proving the beneficial effect of temperature on the system behaviour.

Preprints (www.preprints.org) | NOT PEER-REVIEWED | Posted: 27 January 2023 doi:10.20944/preprints202301.0499.v1

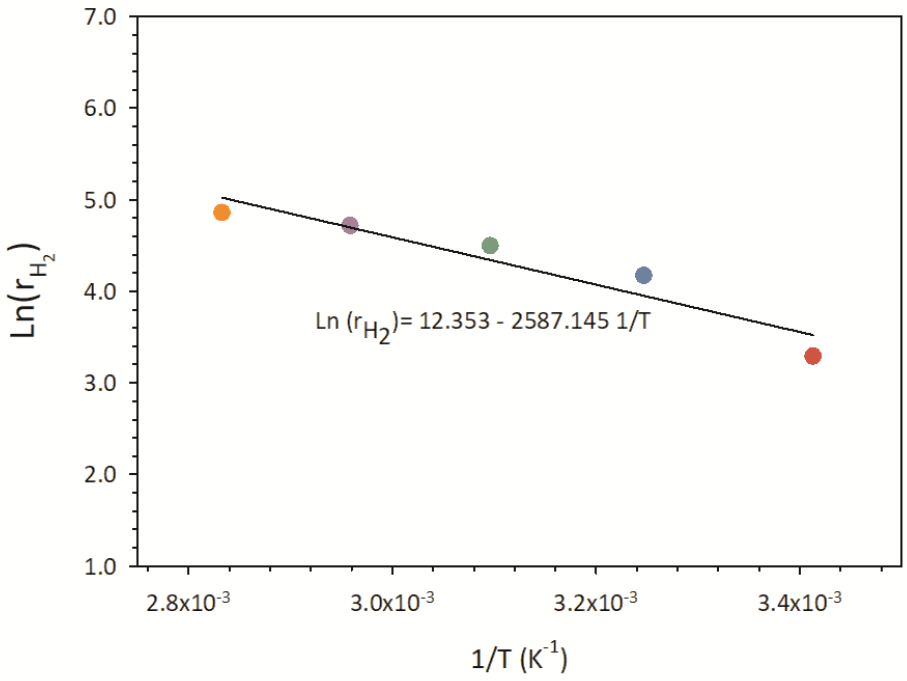

Figure 7. Arrhenius plot for (1%wt.)Cu_2O/TiO_2 photocatalyst.

By considering that the photocatalytic hydrogen production follows a pseudo-first-order law for all the temperatures tested, it is possible to plot the Arrhenius-type equation from 293 K to 353 K (See Figure 7). A value of 21.51 KJ/mol is easily estimated for the apparent activation energy E_a from the slope of the Arrhenius plot. Such a value is consistent with those reported in the literature survey for similar systems [46,47].

Preprints (www.preprints.org) | NOT PEER-REVIEWED | Posted: 27 January 2023 doi:10.20944/preprints202301.0499.v1

Effect of the sacrificial agent

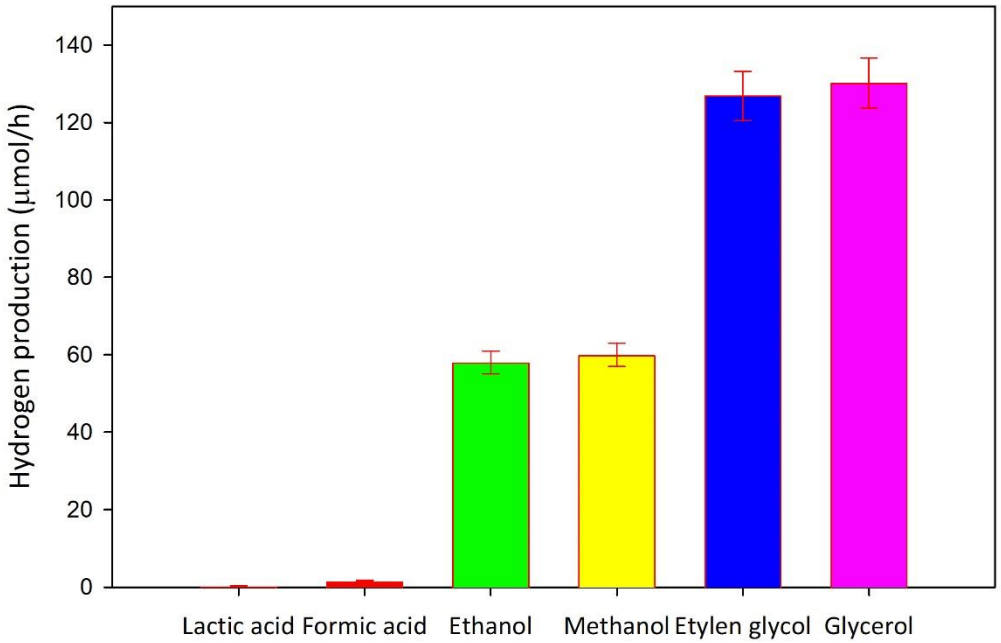

Figure 8. Hydrogen evolution in the presence of various organic species. Experimental conditions: V=0.30 L; P=1 atm; T= 35°C; [Organic] = 2.5 M; $C_{(1\%wt.)Cu2O/TiO2}$ = 700 ppm; visible light radiation.

Many researchers proposed hydrogen production through photoreforming of organics in aqueous phase [14–16]. Organic species may derive from renewable sources or organic-rich effluents [48–50]. Due to (i) the possibility of linking hydrogen generation with water treatment and (ii) the cheap cost of the feedstock, the potential use of organic contaminants found in wastewater is particularly appealing [48,51–53]. Evaluating the effect of the scavenger used on photocatalytic hydrogen production is thus necessary. To this aim, some experimental runs are carried out at varying the sacrificial species (i.e., alcohols or carboxylic acids). The main results collected during this investigation are reported in the Figure 8. Glycerol and 1,2–Ethandiol result the greatest options for hydrogen generation in presence of Cu_2O/TiO_2 photocatalyst, according with literature findings in which Cu-based TiO_2 was used to generate hydrogen through photoreforming [37]. On the contrary, no hydrogen production is herein detected in case of pure water and seawater. Both the nucleophilicity of the groups in the molecular structure of the sacrificial agents and the capacity of the organics to adsorb on the catalyst surface affect the reactivity of the organics with photogenerated hole and can be used to explain these findings. The four species exhibiting the higher photoefficiency for hydrogen evolution (i.e., methanol, ethanol, glycerol and 1,2-ethanediol) have similar values of nucleophilicity, as reported the Table 1. As regards the adsorption

Preprints (www.preprints.org) | NOT PEER-REVIEWED | Posted: 27 January 2023 doi:10.20944/preprints202301.0499.v1

phenomenon, the development of the bidentate (and tridentate) complexes can be proposed for glycerol and 1,2-ethanediol. On the other hand, the creation of weaker monodentate complexes can be supposed for ethanol and methanol, according to their structures.

Table 1.pKa values of several compounds used in the experiments.

Organic species	pKa value	Natural pH of the solution	Reference
Ethanol	15.9	7.0	[54]
Methanol	15.3	8.5	[39]
1,2-ethanediol	15.1	6.0	[39]
Glycerol	14.4	6.5	[39]
Lactic acid	3.86	2.0	[55]
Formic acid	3.75	3.0	[54]

By contrast, the almost negligible photo efficiency for hydrogen evolution recorded in the presence of formic acid and lactic acid can be related to the following phenomena: *(i)* acidic conditions (See Table 1) reduce the stability of copper species, as previously discussed; *(ii)* under acidic conditions, the photocatalyst surface is positively charged, thus exhibiting a weak interaction with the organic compounds. Based on these considerations, glycerol is the best sacrificial agent tested in this study. In addition, a beneficial effect of the temperature on hydrogen evolution is observed also in the case of glycerol. Indeed, when glycerol is used as a scavenger and the system temperature of the system is set at 80°C, the hydrogen generation rate achieves a value of 260 µmol·h^{-1}.

Efficiency calculation

To easily compare the present photocatalytic outcomes with previous findings in the literature survey, the apparent quantum efficiency (AQE) and the light–to–chemical energy efficiency (η) are determined from the best photocatalytic data obtained according to the following equations (eq.4 – eq.5):

$$\text{AQE}\ (\%) = \frac{2 \cdot r_{H_2}}{\text{moles of incident photons/time}} \cdot 100 \qquad \text{eq. 4}$$

$$\eta = \frac{r_{H_2}\ (-\Delta H^0_{comb})}{I \cdot S} \qquad \text{eq. 5}$$

Preprints (www.preprints.org) | NOT PEER-REVIEWED | Posted: 27 January 2023 doi:10.20944/preprints202301.0499.v1

Where:

- r_{H_2} ($mol \cdot s^{-1}$) is the hydrogen generation rate;
- ΔH^0_{comb} is the standard change in enthalpy for the combustion of hydrogen and oxygen ($-282.0 \cdot 10^3$ J/mol);
- I ($W \cdot cm^{-2}$) is the light source's specific irradiance;
- S (cm^2) is the illuminated area.

In Figure 9 the most significant outcomes are reported. When a high–pressure Hg lamp is used, along with a (1%wt) Cu_2O/TiO_2 composite photocatalyst prepared through the ball milling method (200 rpm, 1 min) at a system temperature of 80°C, maximum AQE values of 3.17% and 6.54% are calculated under visible light radiation in presence of methanol and glycerol, respectively. Under identical circumstances, the maximum light–to–chemical energy efficiencies values of 1.16% and 2.36 % are obtained for methanol and glycerol, respectively.

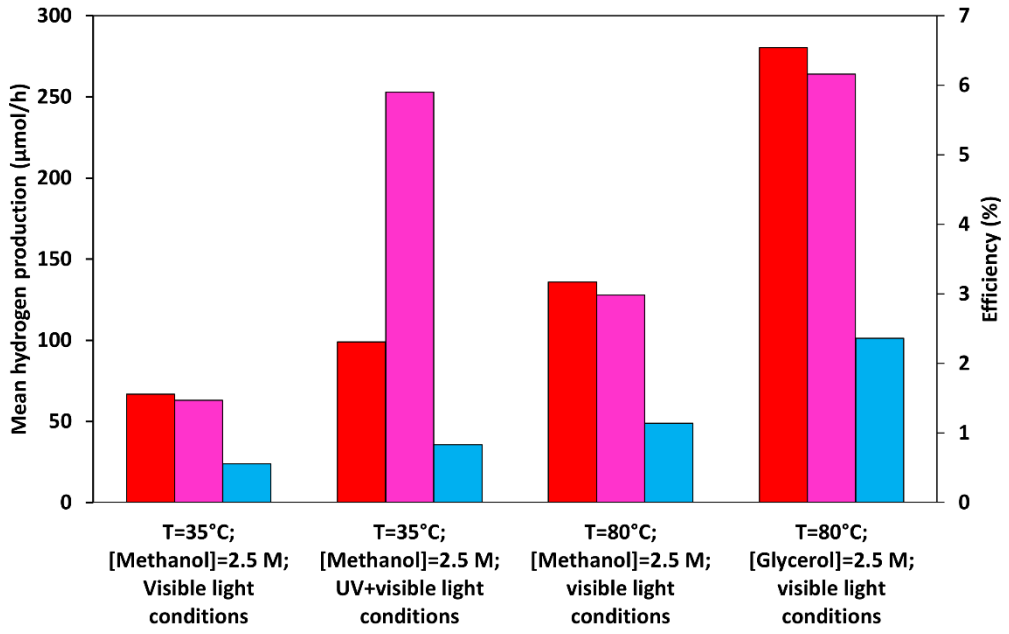

Figure 9. Mean hydrogen generation rate (■), AQE (■), and η (■) obtained under visible light irradiation (λ>400 nm) and UV-A + Visible light conditions.

Additionally, the efficiency values obtained in the visible light spectrum (AQE=1.56%, η=0.56) are only slightly lower than those collected under identical circumstances (T=35°C, methanol as a scavenger) by using UVA+Visible light radiation (AQE=2.31%, η=0.83). In fact, as reported in the figure, despite the huge discrepancy in hydrogen generation in the presence and absence of UVA

Preprints (www.preprints.org) | NOT PEER-REVIEWED | Posted: 27 January 2023 doi:10.20944/preprints202301.0499.v1

radiation, the different light intensities induce comparable activities in terms of quantum yield and light–to–chemical energy efficiency.

Photocatalytic activity under solar conditions

To conclude the experimental campaign of the present study, a set of experiments are performed under direct solar irradiation by using the apparatus schematically represented in the Material and methods section (Figure 1 (B)). Figure 10 reports the main results from the photocatalytic runs conducted under direct solar irradiation.

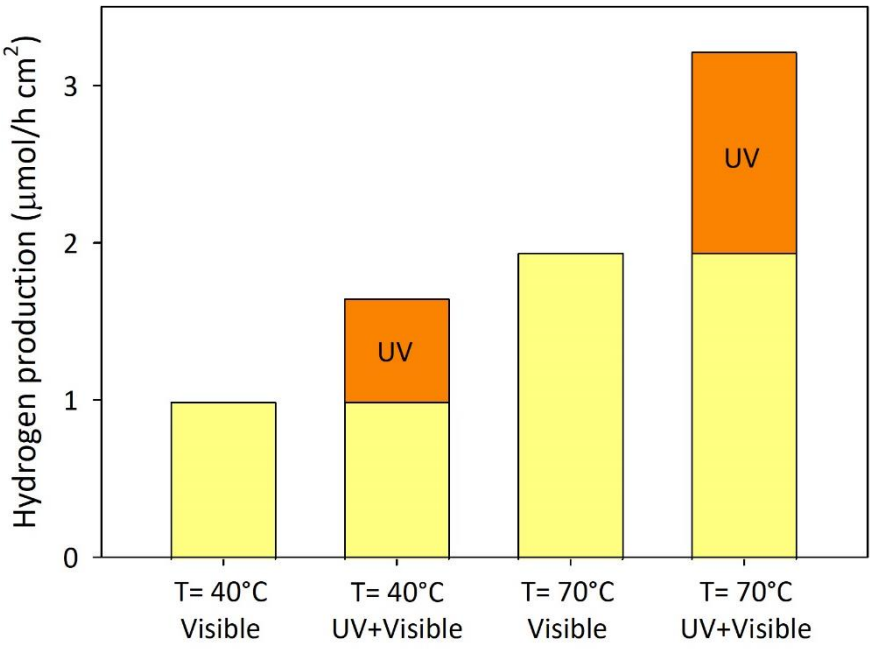

Figure 10. Hydrogen production rate during experimental runs conducted under direct sunlight irradiation. Experimental conditions: V=0.30 L; P=1 atm; pH≈8.5; [MeOH] = 2.5 M; $C_{(1\%wt.)Cu2O/TiO2}$ = 700 ppm.

Hydrogen production rate is about 1 $\mu mol \cdot h^{-1} \cdot cm^{-2}$ at the temperature of 40°C and in the presence of visible light irradiation only. Hydrogen generation increases by about 1.6 times when all wavelengths of the solar spectrum are used. The result indicates that the contribution of the visible light portion of the solar spectrum supports about 60% of hydrogen production under sunlight radiation, whereas the improvement in hydrogen generation obtained without any UV cut-off filter maybe ascribed to the UV component. Furthermore, as the temperature rises to 70°C, the hydrogen generation rate increases to around 3 $\mu mol \cdot h^{-1} \cdot cm^{-2}$, demonstrating the favourable influence of temperature on photocatalytic activity. The efficiencies of the catalytic system adopted in the present investigation for hydrogen generation are calculated by using the irradiance values data collected during the experimental runs. The ranges of irradiation considered are 315–400 nm and

Preprints (www.preprints.org) | NOT PEER-REVIEWED | Posted: 27 January 2023 doi:10.20944/preprints202301.0499.v1

380–550 nm, where the mean values of the specific irradiances are about 15.56 $W \cdot m^{-2}$ and 95.75 $W \cdot m^{-2}$, respectively. Table 3 reports the values of the light to chemical energy efficiency. A value of about 6.5% is obtained considering the contribution of the UV range at a system temperature of 70°C. As regards the light-to-chemical energy efficiency in the solar range, the low calculated values may result from an overestimation of the specific irradiance collected under the visible range (380 – 550 nm). Indeed, wavelengths higher than about 420 nm are completely useless for the activation of the adopted photocatalyst due to its bandgap value (i.e., 3 eV).

Table 2. Mean hydrogen production rate and light-to-chemical energy efficiency (in the UV and the visible range) obtained using the milled catalyst ($C_{(1\%wt.)Cu2O/TiO2}$) under direct sunlight irradiation.

Experimental conditions	η(%) in the UV range	η(%)in the solar range explored
T=40°C; P= 1 atm; pH≈8.5; $C_{(1\%wt.)Cu2O/TiO2}$ = 700 ppm; [Methanol]=2.5 M; Solar light	3.33	1.16
T=70°C; P= 1 atm; pH≈8.5; $C_{(1\%wt.)Cu2O/TiO2}$ = 700 ppm; [Methanol]=2.5 M; Solar light	6.47	2.22

Activity under the best conditions

Eventually, the light-to-chemical energy efficiency is also estimated under the best conditions recorded in the previous sections. In particular, some photocatalytic experiments are carried out under direct sunlight radiation by fixing *(i)* the temperature of the system at 80°C, *(ii)* the pH of the suspension at 12.0, and *(iii)* glycerol as a scavenger. Under these conditions, η reached a value of 8.15% in the UV range, and 2.81% in the visible light range only.

2. Proposed mechanism under solar radiation

Preprints (www.preprints.org) | NOT PEER-REVIEWED | Posted: 27 January 2023 doi:10.20944/preprints202301.0499.v1

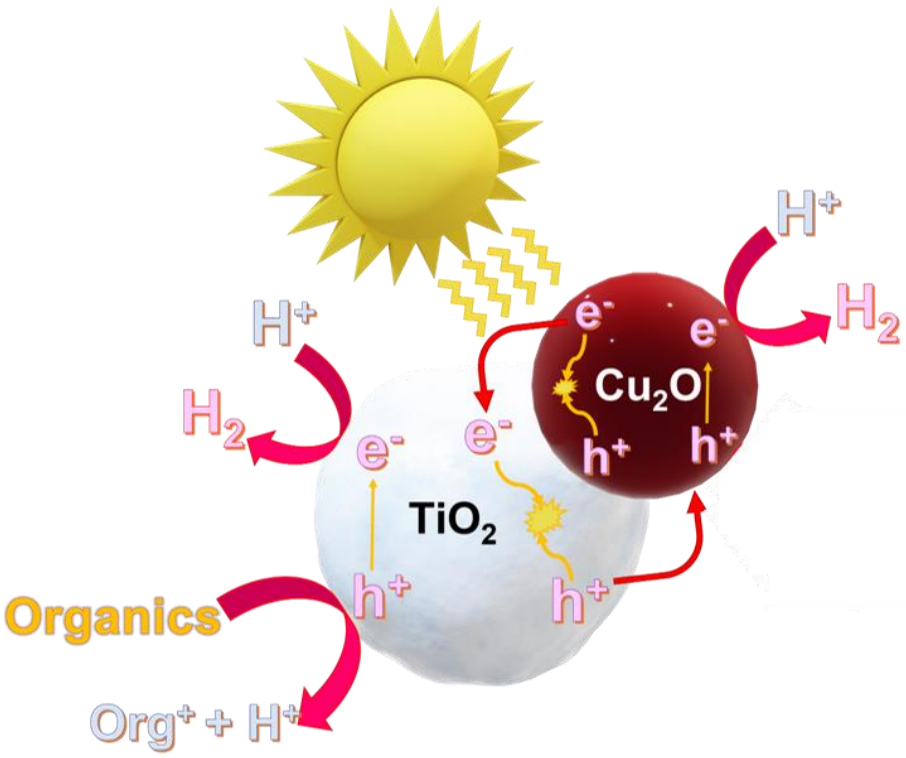

Figure 11. Schematic illustration of the proposed mechanism for hydrogen generation under solar light radiation in presence of Cu_2O/TiO_2 composite material.

An attempt to explain the mechanism of hydrogen generation is herein proposed and discussed (See Figure 11). As previously reported, cuprous oxide in the p–n heterojunction systems based Cu_2O/TiO_2 photocatalysts acts as an energy antenna [27], being able to absorb energy within the visible spectrum. Under direct sunlight radiation, in which the UV and the visible components are present, the activation of both semiconductors (i.e., Cu_2O and TiO_2) can be considered (See the reactions r. 2 and r.3):

$$Cu_2O \xrightarrow{h\nu} Cu_2O(h^+) + Cu_2O(e^-) \qquad \text{r. 2}$$

$$TiO_2 \xrightarrow{h\nu} TiO_2(h^+) + TiO_2(e^-) \qquad \text{r. 3}$$

After charge carrier generation, an electric field from TiO_2 to Cu_2O and band bending are established. Positive holes can react with the adsorbed organic species (mainly on the titania surface), following the reactions r.4 and r.5, thus forming byproducts and protons, which in turn can react with the photogenerated electrons to form $H_{2(g)}$ (through the reaction r.6).

$$Org + \theta_{TiO_2} \overset{K_{ads}}{\longleftrightarrow} Org_{ads} \qquad \text{r. 4}$$

Preprints (www.preprints.org) | NOT PEER-REVIEWED | Posted: 27 January 2023 doi:10.20944/preprints202301.0499.v1

$$Org_{ads} + TiO_2(h^+) \xrightarrow{k_{h^+}} Org^{\bullet}_{ads} + TiO_2(h^+) + H^+ \xrightarrow{Fast} P + 2H^+ \quad \text{r. 5}$$

$$2H^+ + 2TiO_2(e^-) \xrightarrow{Fast} 2H^{\bullet} \xrightarrow{Fast} H_2 \quad \text{r. 6}$$

Obviously, electron-hole pairs may recombine to produce heat and light (through reactions r.7 and r.8), despite the p-n heterojunction formation boosts photogenerated charge carrier separation, resulting in better photocatalytic efficiencies with respect to those observed with bare materials.

$$TiO_2(h^+) + TiO_2(e^-) \xrightarrow{k_r} Q + light \quad \text{r. 7}$$

$$Cu_2O(h^+) + Cu_2O(e^-) \xrightarrow{k_r} Q + light \quad \text{r. 8}$$

Conclusions

The evaluation of the photocatalytic activity for hydrogen generation of the best performing photocatalyst at varying organic concentration allows the identification of an adsorption equilibrium constant of 0.22 M^{-1}. A beneficial effect effect is recorded with raising the system temperature, with an increase in hydrogen productivity of nearly 4.5 times with respect to the lowest temperature. Such a temperature effect is related to the higher reaction rate of hydrogen generation and the easier desorption of the products from the catalyst. As regards the effect of solution pH, alkaline conditions exert beneficial effect on the photocatalytic hydrogen generation. Under the best conditions tested (i.e., glycerol as scavenger, pH=12.0, T=80°C, and direct sunlight irradiation), a value of light-to-chemical energy efficiency of 8% in the UV range is observed. Therefore, the simple photocatalytic system is suited to the visible light driven hydrogen generation. Despite the good performances detected under visible light irradiation only, the UV component in the solar spectrum is able to rise by 40% the photocatalytic hydrogen generation with respect to the visible light irradiation only.

References

1. Ford, A.; Gillich, A.; Mirzania, P. Sustainable Energy and Energy Ef Fi Cient Technologies. **2020**, 611–630, doi:10.1016/B978-0-08-102886-5.00028-1.

2. Li, X.; Liu, B.; Chen, Y.; Fan, X.; Li, Y.; Zhang, F.; Zhang, G.; Peng, W. Decoration of Cu2O Photocathode with Protective TiO2 and Active WS2 Layers for Enhanced Photoelectrochemical Hydrogen Evolution. *Nanotechnology* **2018**, *29*, doi:10.1088/1361-6528/aae569.

3. Hosseini, S.E.; Wahid, M.A. Hydrogen Production from Renewable and Sustainable Energy Resources: Promising Green Energy Carrier for Clean Development. *Renewable and Sustainable Energy Reviews* **2016**, *57*, 850–866, doi:10.1016/j.rser.2015.12.112.

4. Hosseini, S.E. Hydrogen from Solar Energy , a Clean Energy Carrier from a Sustainable Source of Energy. **2019**, 1–22, doi:10.1002/er.4930.

5. Møller, K.T.; Jensen, T.R.; Akiba, E. Progress in Natural Science : Materials International Hydrogen - A Sustainable Energy Carrier. *Progress in Natural Science: Materials International* **2017**, *27*, 34–40, doi:10.1016/j.pnsc.2016.12.014.

6. Policastro, G.; Cesaro, A.; Fabbricino, M. Photo-Fermentative Hydrogen Production from Cheese Whey: Engineering of a Mixed Culture Process in a Semi-Continuous, Tubular Photo-Bioreactor. *Int J Hydrogen Energy* **2022**, doi:10.1016/j.ijhydene.2022.07.063.

7. Policastro, G.; Carraturo, F.; Compagnone, M.; Guida, M.; Fabbricino, M. Enhancing Hydrogen Production from Winery Wastewater through Fermentative Microbial Culture Selection. *Bioresour Technol Rep* **2022**, *19*, doi:10.1016/j.biteb.2022.101196.

8. Kumaravel, V.; Mathew, S.; Bartlett, J.; Pillai, S.C. Photocatalytic Hydrogen Production Using Metal Doped TiO2: A Review of Recent Advances. *Appl Catal B* **2019**, *244*, 1021–1064, doi:10.1016/j.apcatb.2018.11.080.

9. Clarizia, L. Hydrogen Production through Photoreforming of Oxygenated Organic Substrates over Cu/TiO2 Catalysts. **2017**, 1–154.

10. Jing, D.; Guo, L.; Zhao, L.; Zhang, X.; Liu, H.; Li, M.; Shen, S.; Liu, G.; Hu, X.; Zhang, X.; et al. Efficient Solar Hydrogen Production by Photocatalytic Water Splitting: From Fundamental Study to Pilot Demonstration. *Int J Hydrogen Energy* **2010**, *35*, 7087–7097, doi:10.1016/j.ijhydene.2010.01.030.

11. Gong, J.; Li, C.; Wasielewski, M.R. Advances in Solar Energy Conversion. *Chem Soc Rev* **2019**, *48*, 1862–1864, doi:10.1039/c9cs90020a.

12. Kar, S.K.; Sharma, A.; Roy, B. Solar Energy Market Developments in India. *Renewable and Sustainable Energy Reviews* **2016**, *62*, 121–133, doi:10.1016/j.rser.2016.04.043.

13. Shaner, M.R.; Atwater, H.A.; Lewis, N.S.; McFarland, E.W. A Comparative Technoeconomic Analysis of Renewable Hydrogen Production Using Solar Energy. *Energy Environ Sci* **2016**, *9*, 2354–2371, doi:10.1039/c5ee02573g.

14. Christoforidis, K.C.; Fornasiero, P. Photocatalytic Hydrogen Production: A Rift into the Future Energy Supply. *ChemCatChem* **2017**, *9*, 1523–1544, doi:10.1002/cctc.201601659.

15. Lucchetti, R.; Onotri, L.; Clarizia, L.; Natale, F. di; Somma, I. di; Andreozzi, R.; Marotta, R. Removal of Nitrate and Simultaneous Hydrogen Generation through Photocatalytic Reforming of Glycerol over “in Situ” Prepared Zero-Valent Nano Copper/P25. *Appl Catal B* **2017**, *202*, 539–549, doi:https://doi.org/10.1016/j.apcatb.2016.09.043.

16. Miwa, T.; Kaneco, S.; Katsumata, H.; Suzuki, T.; Ohta, K.; Chand Verma, S.; Sugihara, K. Photocatalytic Hydrogen Production from Aqueous Methanol Solution with CuO/Al2O3/TiO2 Nanocomposite. *Int J Hydrogen Energy* **2010**, *35*, 6554–6560, doi:10.1016/j.ijhydene.2010.03.128.

17. Yang, G.; Jiang, Z.; Shi, H.; Xiao, T.; Yan, Z. Preparation of Highly Visible-Light Active N-Doped TiO2 Photocatalyst. *J Mater Chem* **2010**, *20*, 5301–5309, doi:10.1039/c0jm00376j.

18. Rehman, S.; Ullah, R.; Butt, A.M.; Gohar, N.D. Strategies of Making TiO2 and ZnO Visible Light Active. *J Hazard Mater* **2009**, *170*, 560–569, doi:10.1016/j.jhazmat.2009.05.064.

19. Xu, S.; Feng, D.; Shangguan, W. Preparations and Photocatalytic Properties of Visible-Light-Active Zinc Ferrite-Doped TiO2 Photocatalyst. *The Journal of Physical Chemistry C* **2009**, *113*, 2463–2467, doi:10.1021/jp806704y.

20. Al-Azri, Z.H.N.; Chen, W.T.; Chan, A.; Jovic, V.; Ina, T.; Idriss, H.; Waterhouse, G.I.N. The Roles of Metal Co-Catalysts and Reaction Media in Photocatalytic Hydrogen Production: Performance Evaluation of M/TiO2 Photocatalysts (M = Pd, Pt, Au) in Different Alcohol-Water Mixtures. *J Catal* **2015**, *329*, 355–367, doi:10.1016/j.jcat.2015.06.005.

21. Kumaravel, V.; Mathew, S.; Bartlett, J.; Pillai, S.C. Photocatalytic Hydrogen Production Using Metal Doped TiO2: A Review of Recent Advances. *Appl Catal B* **2019**, *244*, 1021–1064, doi:10.1016/j.apcatb.2018.11.080.

22. Humayun, M.; Raziq, F.; Khan, A.; Luo, W. Modification Strategies of TiO2 for Potential Applications in Photocatalysis: A Critical Review. *Green Chem Lett Rev* **2018**, *11*, 86–102, doi:10.1080/17518253.2018.1440324.

23. Muscetta, M.; Russo, D. Photocatalytic Applications in Wastewater and Air Treatment: A Patent Review (2010–2020). *Catalysts* 2021, *11*.

24. Niu, W.; Moehl, T.; Cui, W.; Wick-Joliat, R.; Zhu, L.; Tilley, S.D. Extended Light Harvesting with Dual Cu2O-Based Photocathodes for High Efficiency Water Splitting. *Adv Energy Mater* **2018**, *8*, 1–8, doi:10.1002/aenm.201702323.

25. Yan, L.; Yang, F.; Tao, C.Y.; Luo, X.; Zhang, L. Highly Efficient and Stable Cu2O–TiO2 Intermediate Photocatalytic Water Splitting. *Ceram Int* **2020**, *46*, 9455–9463, doi:10.1016/j.ceramint.2019.12.206.

26. Le, L.; Wu, Y.; Zhou, Z.; Wang, H.; Xiong, R.; Shi, J. Cu2O Clusters Decorated on Flower-like TiO2 Nanorod Array Film for Enhanced Hydrogen Production under Solar Light Irradiation. *J Photochem Photobiol A Chem* **2018**, *351*, 78–86, doi:https://doi.org/10.1016/j.jphotochem.2017.08.073.

27. Muscetta, M.; Andreozzi, R.; Clarizia, L.; di Somma, I.; Marotta, R. Hydrogen Production through Photoreforming Processes over Cu2O/TiO2 Composite Materials: A Mini-Review. *Int J Hydrogen Energy* **2020**, doi:10.1016/j.ijhydene.2020.07.225.

28. Muscetta, M.; Jitan, S. al; Palmisano, G.; Andreozzi, R.; Marotta, R.; Cimino, S.; di Somma, I. Visible Light – Driven Photocatalytic Hydrogen Production Using Cu2O/TiO2 Composites Prepared by Facile Mechanochemical Synthesis. *J Environ Chem Eng* **2022**, *10*, 107735, doi:10.1016/j.jece.2022.107735.

29. Cheng, P.; Li, W.; Zhou, T.; Jin, Y.; Gu, M. Physical and Photocatalytic Properties of Zinc Ferrite Doped Titania under Visible Light Irradiation. *J Photochem Photobiol A Chem* **2004**, *168*, 97–101, doi:10.1016/j.jphotochem.2004.05.018.

30. Muscetta, M.; Clarizia, L.; Garlisi, C.; Palmisano, G.; Marotta, R.; Andreozzi, R.; Ii, F.; Chimica, I.; Industriale, P. Hydrogen Production upon UV-Light Irradiation of Cu / TiO 2 Photocatalyst in the Presence of Alkanol- Amines. *Int J Hydrogen Energy* **2020**, doi:10.1016/j.ijhydene.2020.07.002.

31. Clarizia, L.; Somma, I. Di; Onotri, L.; Andreozzi, R.; Marotta, R. Kinetic Modeling of Hydrogen Generation over Nano-Cu(s)/TiO2 Catalyst through Photoreforming of Alcohols. *Catal Today* **2017**, *281*, 117–123, doi:10.1016/j.cattod.2016.05.053.

32. Badawy, M.I.; Ghaly, M.Y.; Ali, M.E.M. Photocatalytic Hydrogen Production over Nanostructured Mesoporous Titania from Olive Mill Wastewater. *Desalination* **2011**, *267*, 250–255, doi:10.1016/j.desal.2010.09.035.

33. Lin, W.C.; Yang, W.D.; Huang, I.L.; Wu, T.S.; Chung, Z.J. Hydrogen Production from Methanol/Water Photocatalytic Decomposition Using Pt/Tio2-Xnx Catalyst. *Energy and Fuels* **2009**, *23*, 2192–2196, doi:10.1021/ef801091p.

34. Wu, Y.; Lu, G.; Li, S. The Role of Cu(I) Species for Photocatalytic Hydrogen Generation over CuO x /TiO2. *Catal Letters* **2009**, *133*, 97–105, doi:10.1007/s10562-009-0165-y.

35. Karimi Estahbanati, M.R.; Mahinpey, N.; Feilizadeh, M.; Attar, F.; Iliuta, M.C. Kinetic Study of the Effects of PH on the Photocatalytic Hydrogen Production from Alcohols. *Int J Hydrogen Energy* **2019**, *44*, 32030–32041, doi:10.1016/j.ijhydene.2019.10.114.

36. Corredor, J.; Rivero, M.J.; Rangel, C.M.; Gloaguen, F.; Ortiz, I. Comprehensive Review and Future Perspectives on the Photocatalytic Hydrogen Production. *Journal of Chemical Technology and Biotechnology* 2019, *94*, 3049–3063.

37. Clarizia, L.; Spasiano, D.; di Somma, I.; Marotta, R.; Andreozzi, R.; Dionysiou, D.D. Copper Modified-TiO2 Catalysts for Hydrogen Generation through Photoreforming of Organics. A Short Review. *Int J Hydrogen Energy* **2014**, *39*, 16812–16831, doi:10.1016/j.ijhydene.2014.08.037.

38. Xu, S.; Ng, J.; Zhang, X.; Bai, H.; Sun, D.D. Fabrication and Comparison of Highly Efficient Cu Incorporated TiO 2 Photocatalyst for Hydrogen Generation from Water. *Int J Hydrogen Energy* **2010**, *35*, 5254–5261, doi:10.1016/j.ijhydene.2010.02.129.

39. Serjeant, E.P.; Dempsey, Boyd. *Ionisation Constants of Organic Acids in Aqueous Solution*; International Union of Pure and Applied Chemistry. Commission on Equilibrium Data. IUPAC chemical data series ; no. 23.; Pergamon Press: Oxford ;, 1979; ISBN 0080223397.

40. Kosmulski, M. Isoelectric Points and Points of Zero Charge of Metal (Hydr)Oxides: 50 Years after Parks' Review. *Adv Colloid Interface Sci* **2016**, *238*, 1–61, doi:10.1016/j.cis.2016.10.005.

41. Hu, J.; Wang, J.; Liu, S.; Zhang, Z.; Zhang, H.; Cai, X.; Pan, J.; Liu, J. Effect of TiO2 Nanoparticle Aggregation on Marine Microalgae Isochrysis Galbana. *J Environ Sci (China)* **2018**, *66*, 208–215, doi:10.1016/j.jes.2017.05.026.

42. Gao, M.; Zhang, T.; Ho, G.W. Advances of Photothermal Chemistry in Photocatalysis, Thermocatalysis, and Synergetic Photothermocatalysis for Solar-to-Fuel Generation. *Nano Res* 2022.

43. Reza, M.S.; Ahmad, N.B.H.; Afroze, S.; Taweekun, J.; Sharifpur, M.; Azad, A.K. Hydrogen Production from Water Splitting through Photocatalytic Activity of Carbon-Based Materials. *Chem Eng Technol* 2022.

44. Huaxu, L.; Fuqiang, W.; Ziming, C.; Shengpeng, H.; Bing, X.; Xiangtao, G.; bo, L.; Jianyu, T.; Xiangzheng, L.; Ruiyang, C.; et al. Analyzing the Effects of Reaction Temperature on Photo-Thermo Chemical Synergetic Catalytic Water Splitting under Full-Spectrum Solar Irradiation: An Experimental and Thermodynamic Investigation. *Int J Hydrogen Energy* **2017**, *42*, 12133–12142, doi:10.1016/j.ijhydene.2017.03.194.

45. Zhang, Z.; Maggard, P.A. Investigation of Photocatalytically-Active Hydrated Forms of Amorphous Titania, TiO2·nH2O. *J Photochem Photobiol A Chem* **2007**, *186*, 8–13, doi:10.1016/j.jphotochem.2006.07.004.

46. Song, R.; Luo, B.; Geng, J.; Song, D.; Jing, D. Photothermocatalytic Hydrogen Evolution over Ni2P/TiO2 for Full-Spectrum Solar Energy Conversion. *Ind Eng Chem Res* **2018**, *57*, 7846–7854, doi:10.1021/acs.iecr.8b00369.

47. Velázquez, J.J.; Fernández-González, R.; Díaz, L.; Pulido Melián, E.; Rodríguez, V.D.; Núñez, P. Effect of Reaction Temperature and Sacrificial Agent on the Photocatalytic H2-Production of Pt-TiO2. *J Alloys Compd* **2017**, *721*, 405–410, doi:10.1016/j.jallcom.2017.05.314.

48. Rico-Oller, B.; Boudjemaa, A.; Bahruji, H.; Kebir, M.; Prashar, S.; Bachari, K.; Fajardo, M.; Gómez-Ruiz, S. Photodegradation of Organic Pollutants in Water and Green Hydrogen Production via Methanol Photoreforming of Doped Titanium Oxide Nanoparticles. *Science of the Total Environment* **2016**, *563–564*, 921–932, doi:10.1016/j.scitotenv.2015.10.101.

49. Munusamy, T.D.; Chin, S.Y.; Tarek, M.; Khan, M.M.R. Sustainable Hydrogen Production by CdO/Exfoliated g-C3N4 via Photoreforming of Formaldehyde Containing Wastewater. *Int J Hydrogen Energy* **2021**, *46*, 30988–30999, doi:10.1016/j.ijhydene.2021.01.176.

50. Koca, A.; Ahin, M.S. *Photocatalytic Hydrogen Production by Direct Sun Light from Sulfide=sulfite Solution*; 2002; Vol. 27;.

51. Wei, Z.; Liu, J.; Shangguan, W. A Review on Photocatalysis in Antibiotic Wastewater: Pollutant Degradation and Hydrogen Production. *Chinese Journal of Catalysis* **2020**, *41*, 1440–1450, doi:10.1016/S1872-2067(19)63448-0.

52. Chowdhury, P.; Malekshoar, G.; Ray, M.B.; Zhu, J.; Ray, A.K. Sacrificial Hydrogen Generation from Formaldehyde with Pt/TiO2 Photocatalyst in Solar Radiation. *Ind Eng Chem Res* **2013**, *52*, 5023–5029, doi:10.1021/ie3029976.

53. Zhang, S.; Wang, L.; Liu, C.; Luo, J.; Crittenden, J.; Liu, X.; Cai, T.; Yuan, J.; Pei, Y.; Liu, Y. Photocatalytic Wastewater Purification with Simultaneous Hydrogen Production Using MoS2 QD-Decorated Hierarchical Assembly of ZnIn2S4 on Reduced Graphene Oxide Photocatalyst. *Water Res* **2017**, *121*, 11–19, doi:10.1016/j.watres.2017.05.013.

54. Riddick, J.A.; Bunger, W.B.; Sakano, T.K. *Organic Solvents: Physical Properties and Methods of Purification.*; 4th ed.; Wiley-Interscience: New York, 1986;

55. Williams, M. *The Merck Index: An Encyclopedia of Chemicals, Drugs, and Biologicals*; 15th ed.; Royal Society of Chemistry: Cambridge, UK, 2013;